Tetrahedron 70 (2014) 3935–3942

Contents lists available at ScienceDirect

Tetrahedron

journal homepage: www.elsevier.com/locate/tet

Star-shaped triphenylamine terminated difluoroboron β-diketonate complexes: synthesis, photophysical and electrochemical properties

Chong Qian, Guanghui Hong, Mingyang Liu, Pengchong Xue, Ran Lu *

State Key Laboratory of Supramolecular Structure and Materials, College of Chemistry, Jilin University, Changchun 130012, PR China

ARTICLE INFO

Article history:
Received 30 December 2013
Received in revised form 14 March 2014
Accepted 20 March 2014
Available online 28 March 2014

Keywords:
Star-shaped macromolecules
Triphenylamine
Difluoroboron β-diketonate
Photophysical
Electrochemical

ABSTRACT

Two new star-shaped difluoroboron β-diketonate complexes **(TBC)$_3$Ph** and **(TBF)$_3$Ph**, in which the terminal groups of triphenylamine functionalized difluoroboron β-diketonates were bridged by carbazole or fluorene to the core of 1,3,5-benzene, have been synthesized. It was found that they gave high molar extinction coefficients, meaning strong light-harvesting ability, and emitted intense yellow light with fluorescence quantum yields (Φ_F) of 0.73 and 0.67 for **(TBC)$_3$Ph** and **(TBF)$_3$Ph**, respectively, in toluene as well as red light in solid states with Φ_F of 0.36 and 0.27, respectively. The electrochemical behaviors suggested that they had considerably higher electron affinities than tris(8-hydroxyquinoline)aluminum (AlQ$_3$), which indicated that they could be used as electron-transporting materials besides emitting materials.

1. Introduction

Four-coordinate organoboron complexes have been extensively studied for various applications in biological sensing and imaging, electroluminescent devices, etc.[1–3] Among them, difluoroboron β-diketonate complexes have attracted much interest because of their intriguing properties, such as high quantum yields, large molar extinction coefficients, strong emission in solid state, high electron affinities, and sensitivity to the surrounding medium.[4–7] Therefore, they have been employed in various fields, including two-photon absorption materials,[8] mechanochromic luminescent materials,[9] near-IR probes,[10] and organic field-effect transistors.[11] For example, Fraser's group has synthesized a series of difluoroboron β-diketonate complexes and investigated their reversible mechanochromic fluorescence in solid state.[9] Perry et al. have developed two-photon absorption materials based on difluoroboron β-diketonate complexes, which can be used to photoreduce silver ions.[8b] Additionally, the formation of stable six-membered boron-chelating ring in difluoroboron β-diketonate complexes can inhibit the nonradiative dissipation through O–H stretching modes from tautomerization between ketone and enol forms, and may extend the π-conjugation of the molecules, which would favor the molecular assembly via π–π interaction. Recently, our group reported the facile fabrication of low-dimensional nanostructures from triphenylamine functionalized difluoroboron β-diketonate complexes, which can be used as fluorescent sensory materials for detecting organic amines vapor with high sensitivity and fast response rate.[12] On the other hand, star-shaped π-conjugated systems have attracted considerable attention recently due to their unique properties, such as suppressing the quenching of fluorescence in solid state, improving the light-harvesting ability and so on.[13] They have exhibited potential applications in photovoltaic cells,[14] organic light-emitting diodes,[15] nonlinear optics,[16,17] and field-effect transistors.[18] However, to the best of our knowledge, reports on the construction of star-shaped molecules based on difluoroboron β-diketone derivatives are rare. Herein, in order to gain novel difluoroboron β-diketone complexes with enhanced light-harvesting ability and intensive emission in solution as well as in the solid state, we designed new star-shaped macromolecules **(TBC)$_3$Ph** and **(TBF)$_3$Ph** (Scheme 1), in which the terminal groups of triphenylamine functionalized difluoroboron β-diketonates were bridged by carbazole or fluorene to the core of 1,3,5-benzene. It was found that **(TBC)$_3$Ph** and **(TBF)$_3$Ph** gave high molar extinction coefficients of 2.90×10^5 M^{-1} cm^{-1} and 3.11×10^5 M^{-1} cm^{-1} in THF, respectively, meaning strong light-harvesting ability. Meanwhile, **(TBC)$_3$Ph** and **(TBF)$_3$Ph** not only could emit intense yellow light in toluene with the fluorescence quantum yields (Φ_F) of 0.73 and 0.69, respectively, but also emit strong red light in solid states with Φ_F of 0.36 and 0.27, respectively. The electrochemical data suggested that they had considerably higher electron affinities than tris(8-hydroxyquinoline)aluminum (AlQ$_3$), indicating they might be used as electron-transporting materials besides emitting materials.

---

* Corresponding author. Tel.: +86 431 88499179; fax: +86 431 88923907; e-mail address: luran@mail.jlu.edu.cn (R. Lu).

0040-4020/$ – see front matter © 2014 Elsevier Ltd. All rights reserved.
http://dx.doi.org/10.1016/j.tet.2014.03.069

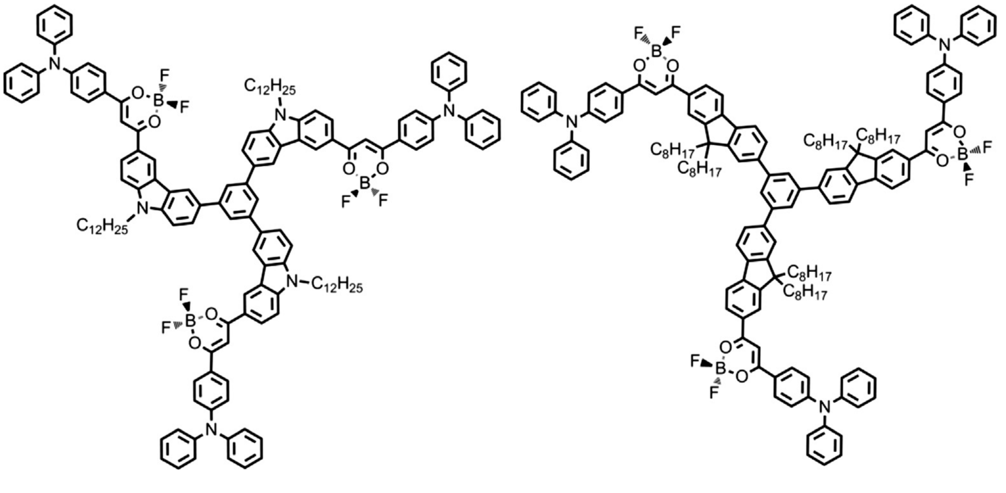

Scheme 1. Molecular structures of (**TBC**)$_3$**Ph** and (**TBF**)$_3$**Ph**.

2. Results and discussion

2.1. Synthesis and characterizations

The synthetic routes for the star-shaped triphenylamine terminated difluoroboron β-diketonate complexes (**TBC**)$_3$**Ph** and (**TBF**)$_3$**Ph** were shown in Scheme 2. Firstly, compound **2** was synthesized via Friedel–Crafts acylation reaction of compound **1** with acetyl chloride in a yield of 52%. Then, the Suzuki coupling reaction between compound **2** and 1,3,5-tris(4,4,5,5-tetramethyl-1,3,2-dioxaborolan-2-yl)benzene gave compound **3** in a yield of 27%. The Claisen condensation between methyl 4-(diphenylamino) benzoate and compound **3** in the presence of sodium hydride in anhydrous toluene yielded 3,3′,3″-(6,6′,6″-(benzene-1,3,5-triyl) tris(9-dodecyl-9*H*-carbazole-6,3-diyl))tris(1-(4-(diphenylamino) phenyl)propane-1,3-dione), which was not further purified and complexed with boron trifluoride–diethyl etherate directly in anhydrous CH_2Cl_2, affording (**TBC**)$_3$**Ph** in a yield of 18%. Similarly, compound **5** was gained from compound **4** through Friedel–Crafts acylation reaction, and it was transferred into compound **6** under Suzuki coupling reaction condition in a yield of 35%. Finally, 3,3′,3″-(benzene-1,3,5-triyltris(9,9-dioctyl-9*H*-fluorene-7,2-diyl))tris(1-(4-(diphenylamino)phenyl)propane-1,3-dione) was prepared via the Claisen condensation reaction between methyl 4-(diphenylamino)benzoate and compound **6**, and it complexed with boron trifluoride–diethyl etherate directly to give (**TBF**)$_3$**Ph** in a yield of 12% over two steps. The new compounds were characterized by ^{1}H NMR, ^{13}C NMR, MALDI-TOF mass spectrometry, and C, H, N elemental analyses. And two complexes are air-stable and show good solubility in THF, CH_2Cl_2, $CHCl_3$, DMSO, ethyl acetate, and aromatic solvents (such as benzene and toluene), while they have poor solubility in alcohols (such as ethanol and methanol) and aliphatic hydrocarbon solvents (such as petroleum ether and *n*-hexane).

2.2. UV–vis absorption and fluorescent emission spectra

The UV–vis absorption and the fluorescence emission spectra of (**TBC**)$_3$**Ph** and (**TBF**)$_3$**Ph** in toluene and in the films were shown in Fig. 1, and the corresponding photophysical data were summarized in Table 1. It was clear that (**TBC**)$_3$**Ph** showed several obvious

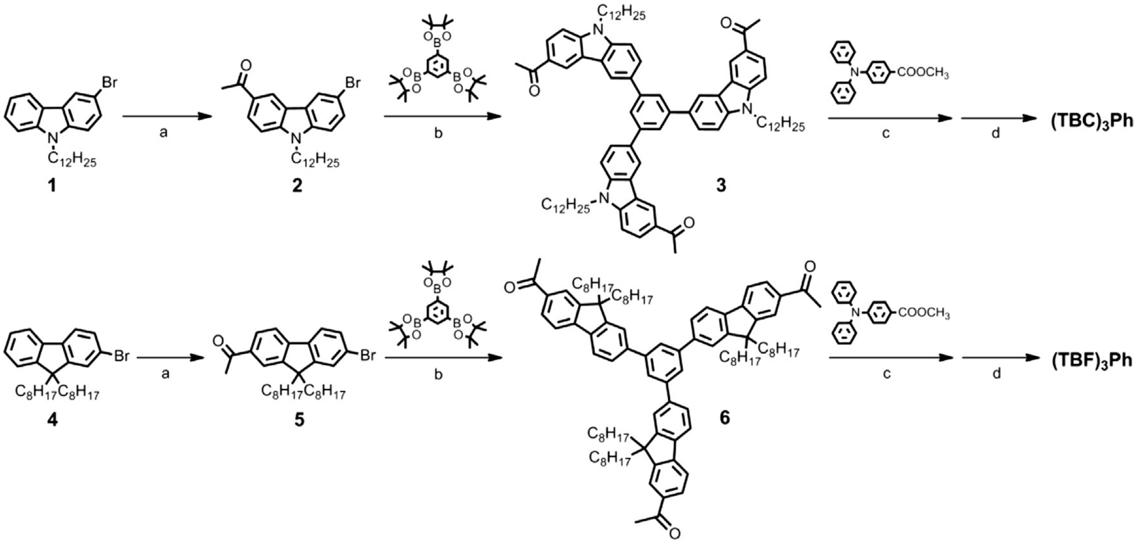

(a) CH_3COCl, $AlCl_3$, $ClCH_2CH_2Cl$; (b) $Pd(PPh_3)_4$, K_2CO_3, Toluene/H_2O; (c) NaH, Toluene; (d) $BF_3{\cdot}Et_2O$, CH_2Cl_2.

Scheme 2. Synthetic routes for complexes (**TBC**)$_3$**Ph** and (**TBF**)$_3$**Ph**.

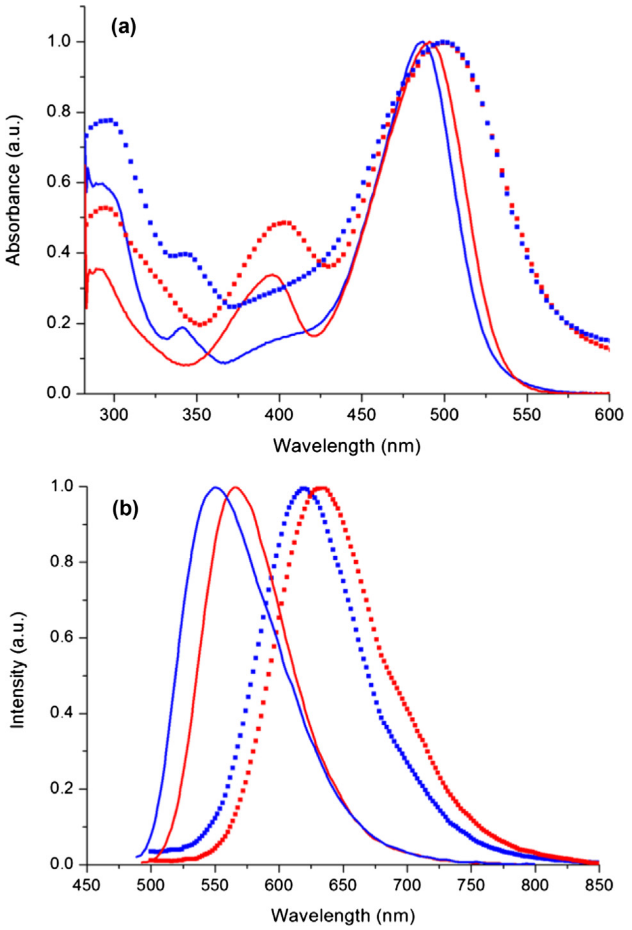

Fig. 1. Normalized UV–vis absorption (a) and fluorescence emission (b, λ_{ex}=486 nm) spectra of (**TBC**)$_3$**Ph** (blue) and (**TBF**)$_3$**Ph** (red) in toluene (solid, 2.0×10^{-6} M) and in the films (dashed).

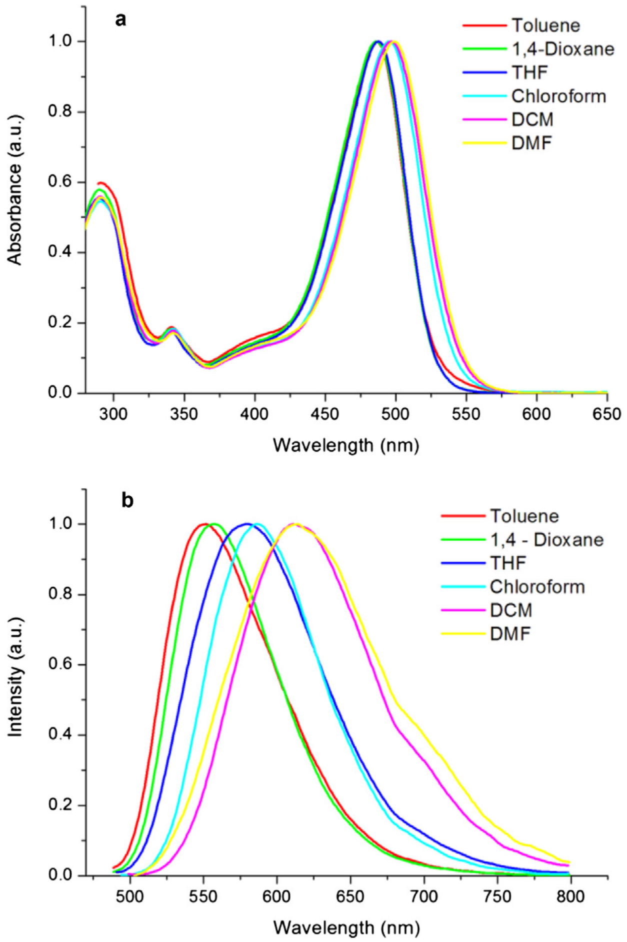

Fig. 2. Normalized UV–vis absorption (a) and fluorescence emission spectra (b, λ_{ex}=486 nm) of (**TBC**)$_3$**Ph** in different solvents (2.0×10^{-6} M).

Table 1
Photophysical data of (**TBC**)$_3$**Ph** and (**TBF**)$_3$**Ph** in different solvents

Complex	Solvents	λ_{abs}^{max}/nm (ε_{max}[a])	λ_{em}/nm	$\Delta\nu_{st}$[b]/cm^{-1}	Φ_F[c]
(**TBC**)$_3$**Ph**	Toluene	486 (2.49)	551	2427	0.73
	1,4-Dioxane	486 (2.81)	556	2590	0.69
	THF	488 (2.90)	580	3250	0.33
	Chloroform	496 (3.07)	588	3154	0.51
	DCM	496 (2.85)	611	3794	0.15
	DMF	497 (2.77)	615	4148	0.02
(**TBF**)$_3$**Ph**	Toluene	490 (2.76)	566	2740	0.67
	1,4-Dioxane	489 (3.01)	588	3443	0.51
	THF	490 (3.11)	617	4201	0.08
	Chloroform	496 (2.14)	622	4084	0.24
	DCM	497 (3.05)	648	4689	0.03
	DMF	500 (3.01)	664	4939	—

[a] $\times10^5$ M^{-1} cm^{-1}.
[b] $\Delta\nu_{st}=\nu_{abs}-\nu_{em}$.
[c] Fluorescence quantum yield determined by a standard method with Rhodamine 6G in water (Φ_F=0.75, λ_{ex}=488 nm) as reference.

absorption bands in toluene from 290 nm to 600 nm (Fig. 1a). The bands appeared at 290 nm and 342 nm were due to the electronic transitions of triphenylamine and carbazole units, the one at ca. 400 nm was assigned to the $\pi-\pi^*$ transition of the molecule, and the band emerged at 486 nm was ascribed to the intermolecular charge transfer (ICT) transition, which could be supported by the solvent-dependent absorption and fluorescence emission spectral changes (Fig. 2 and Table 1). For example, the maximal absorption band of (**TBC**)$_3$**Ph** located at 486 nm in toluene red-shifted gradually with increasing the polarity of the solvents, and it reached 497 nm in DMF (Fig. 2a). These results suggest an excited state with a larger dipole moment than that in the ground state.[19] Moreover, the fluorescence emission bands of (**TBC**)$_3$**Ph** red-shifted significantly with increasing the solvent polarity, accompanying with the broaden of the emission. For example, the emission maximum of (**TBC**)$_3$**Ph** in toluene appeared at 551 nm (Fig. 1b), which red-shifted to 615 nm in DMF (Fig. 2b). Therefore, such significant red-shift and the broaden of the emission band with increasing the polarity of the solvents indicated the ICT emission feature of (**TBC**)$_3$**Ph**.[12] It should be noted that (**TBC**)$_3$**Ph** gave high molar extinction coefficient (ε_{max}) of 2.90×10^5 M^{-1} cm^{-1} in THF, which was nearly three times as high as our previously reported similar difluoroboron β-diketonate complex **BDOBC16** (1.0×10^5 M^{-1} cm^{-1} in THF).[12d] Therefore, the star-shaped structure can remarkably improve the light-harvesting ability of difluoroboron β-diketonate complex, which is of importance in light-harvesting systems.[14] On the other hand, the absorption and emission behaviors of (**TBF**)$_3$**Ph** were similar to those of (**TBC**)$_3$**Ph**. The ε_{max} for (**TBF**)$_3$**Ph** reached 3.11×10^5 M^{-1} cm^{-1} in THF. The maximal absorption and emission bands for (**TBF**)$_3$**Ph** emerged at 490 nm and 566 nm in toluene, respectively, giving a little red-shift compared with those for (**TBC**)$_3$**Ph** (486 nm and 551 nm, respectively) due to the larger molecular π-conjugation of (**TBF**)$_3$**Ph** bearing the linker of 2,7-fluorene than that in (**TBC**)$_3$**Ph** bearing the spacer of 3,6-carbazole.[20] We also confirmed that the above bands also resulted from ICT transition (Figs. 1 and 2, Fig. S1, and Table 1). In addition, it should be noted that the maximal absorption of

(TBC)$_3$Ph and **(TBF)$_3$Ph** in the films became broad and showed a red-shift of 14 nm and 10 nm, respectively, compared with those in toluene on account of the aromatic π-stacking interaction in solid states, and the smaller red-shift of the absorption band for **(TBF)$_3$Ph** compared with that in **(TBC)$_3$Ph** might result from a better site-isolation effect of the branched alkyl group in fluorene.[21] Meanwhile, the emission band of **(TBF)$_3$Ph** red-shifted to 632 nm in the film from 566 nm in toluene ($\Delta\lambda$=66 nm), and that of **(TBC)$_3$Ph** red-shifted to 619 nm in the film from 551 nm in toluene ($\Delta\lambda$=68 nm), further indicating the better site-isolation effect in star-shaped **(TBF)$_3$Ph**. Furthermore, the fluorescence quantum yields of the two complexes in different solvents were determined using Rhodamine 6G as standard. We found that the Φ_F values of **(TBC)$_3$Ph** and **(TBF)$_3$Ph** were 0.73 and 0.67 in toluene, respectively, meaning that they were strong emissive in non-polar solvents, and they decreased with the increasing the solvent polarity (Table 1) because of the decreased radiative decay process. Moreover, the fluorescence quantum yields of **(TBC)$_3$Ph** and **(TBF)$_3$Ph** in solid states were measured using an integrating sphere, and they were 0.36 and 0.27, respectively, suggesting strong emissive in solid states. Therefore, the strong emission for the star-shaped difluoroboron β-diketonate in solid states made it possible to be applied as emitting materials in organic light-emitting diodes.

2.3. Electrochemical properties

The electrochemical behaviors were investigated by cyclic voltammetry. It was clear that **(TBC)$_3$Ph** and **(TBF)$_3$Ph** gave one well-defined reversible reduced peak with half-wave potential ($E^{1/2}_{\text{red}}$) of -1.59 and -1.48 V versus ferrocenium/ferrocene (Fig. 3). Compared with **(TBF)$_3$Ph**, the $E^{1/2}_{\text{red}}$ of **(TBC)$_3$Ph** showed a slight negative shift due to the electron-donating effect of carbazole. Nonetheless, they had considerably higher electron affinities than AlQ$_3$ (ca. -2.30 V in 1/1 acetonitrile/benzene[22]), so they might have potential applications as electron-transport materials.[23] The redox potential of Fc/Fc$^+$, which possesses an absolute energy level of 4.8 eV relative to the vacuum level for calibration, is located at 0.22 eV in our case. Therefore, the LUMO energy levels of **(TBC)$_3$Ph** and **(TBF)$_3$Ph** were calculated to be -3.21 eV and -3.32 eV with regard to ferrocene.[24] Because no clear oxidation waves were observed, the HOMO energy levels were deduced to be -5.48 eV and -5.55 eV from LUMO energy levels and energy gaps determined by the onset of their absorption spectra. The corresponding data were summarized in Table 2.

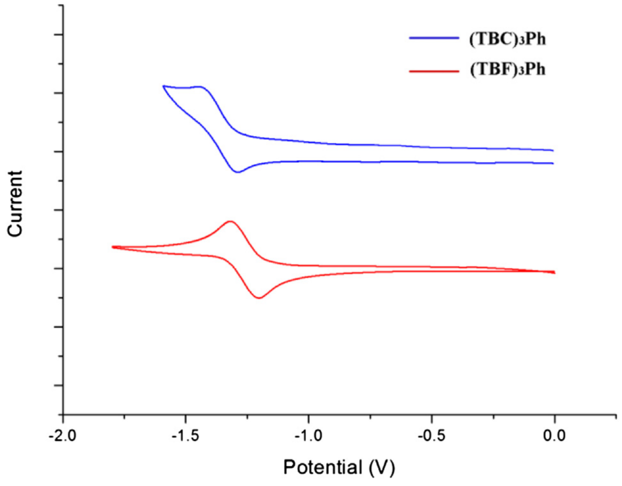

Fig. 3. Cyclic voltammograms of **(TBC)$_3$Ph** and **(TBF)$_3$Ph** in CH$_2$Cl$_2$.

Table 2
Electrochemical and theoretical calculated data

Complex	$E^{1/2}_{\text{red}}$[a] (V)	HOMO[b] (eV)	LUMO[b] (eV)	E_g[c] (eV)	HOMO[d] (eV)	LUMO[d] (eV)
(TBC)$_3$Ph	−1.59	−5.48	−3.21	2.27	−5.32	−2.42
(TBF)$_3$Ph	−1.48	−5.55	−3.32	2.23	−5.57	−2.76

[a] $E^{1/2}_{\text{red}}$ (V)=onset reduction potential, Potentials are given against ferrocenium/ferrocene.
[b] Calculated using the empirical equation: LUMO=$-(4.8+E^{1/2}_{\text{red}})$ and $E_{\text{HOMO}}=E_{\text{LUMO}}-E_g$.
[c] Estimated from the onset of the absorption spectra (E_g=1240/λ_{onset}).
[d] Obtained from quantum chemical calculation using DFT/B3LYP/6-31G.

2.4. Theoretical calculations

To gain an insight into the photophysical and electrochemical properties of these two star-shaped complexes at the molecular level, density functional theory (DFT) was used to calculate the electronic structures and time-dependent DFT (TD-DFT) was adopted to investigate the electronic transitions from ground to excitation states. All calculations were performed at B3LYP/6-31G level with the Gaussian 09W program package.[25] Fig. 4 showed the plots of molecular orbitals involved in the electronic transitions of **(TBC)$_3$Ph**. In the optimized structure of **(TBC)$_3$Ph**, the π-electrons in HOMO (highest occupied molecular orbital) and HOMO-1 were mainly delocalized over the triphenylamine and carbazole units, and those in HOMO-2 were mainly delocalized over the triphenylamine unit, while LUMO (lowest unoccupied molecular orbital), LUMO+1 and LUMO+2 were mainly delocalized over difluoroboron β-diketone moieties. Similarly, the LUMO, LUMO+1, and LUMO+2 of **(TBF)$_3$Ph** were also mainly delocalized over the acceptor of difluoroboron β-diketone moiety (Fig. 5). However, the π-electron in the HOMO, HOMO-1, and HOMO-2 of **(TBF)$_3$Ph** was mainly delocalized over triphenylamine units except for fluorene unit due to its weaker electron donating ability than carbazole in **(TBC)$_3$Ph**. On the other hand, the electronic transition bands of **(TBC)$_3$Ph** and **(TBF)$_3$Ph** calculated by TD-DFT were listed in Table 3. For **(TBC)$_3$Ph**, we could find two calculated electronic transition bands at 484.4 nm and 482.8 nm from Fig. S2, which originated from several transitions of HOMO/HOMO-2 to LUMO, HOMO-1 to LUMO+1, and HOMO/HOMO-1/HOMO-2 to LUMO+2. Moreover, we deduced that the maximum absorption band at 486 nm of **(TBC)$_3$Ph** (in toluene) detected in UV–vis absorption spectrum corresponded to the above calculates ones. Combined with the characters of HOMO-2, HOMO-1, HOMO, LUMO, LUMO+1, LUMO+2, the absorption at 486 nm could be assigned to ICT transition.[26] Similarly, the absorption band at 490 nm of **(TBF)$_3$Ph** in toluene was also relevant to the two calculated bands at 494.4 nm and 493.5 nm (Fig. S3) coming from ICT transitions. Therefore, the maximum absorption of **(TBC)$_3$Ph** and **(TBF)$_3$Ph** resulted from an ICT transition, which was consistent with the results of UV–vis absorption and fluorescent emission.[5,27,28]

3. Conclusions

In summary, we synthesized novel star-shaped difluoroboron β-diketonate complexes **(TBC)$_3$Ph** and **(TBF)$_3$Ph**, in which the terminal groups of triphenylamine functionalized difluoroboron β-diketonates were bridged by carbazole or fluorene to the core of 1,3,5-benzene. It was found that they gave high molar extinction coefficients, for example, the $\varepsilon_{\max}$ of **(TBF)$_3$Ph** reached 3.11×10^5 M^{-1} cm^{-1} in THF, which was higher than other reported difluoroboron β-diketonate complexes and meant strong light-harvesting ability of the synthesized star-shaped macromolecules. Meanwhile, **(TBC)$_3$Ph** and **(TBF)$_3$Ph** emitted intense yellow light in

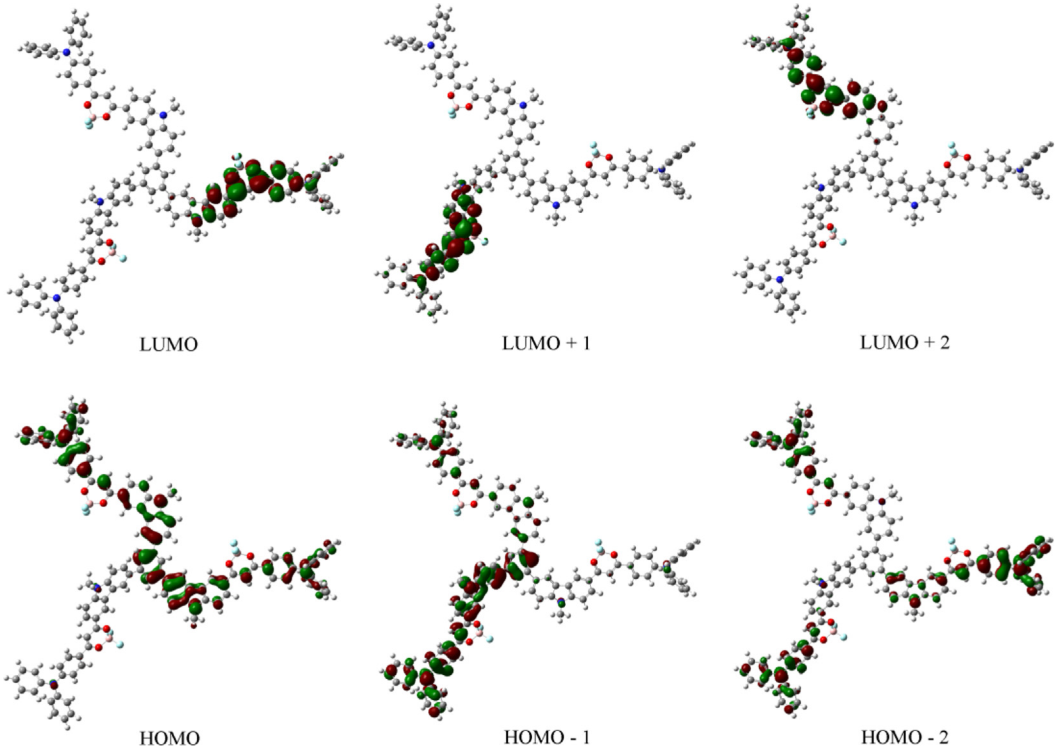

Fig. 4. The molecular orbital surfaces in the optimized ground-state structure for (**TBC**)$_3$**Ph**.

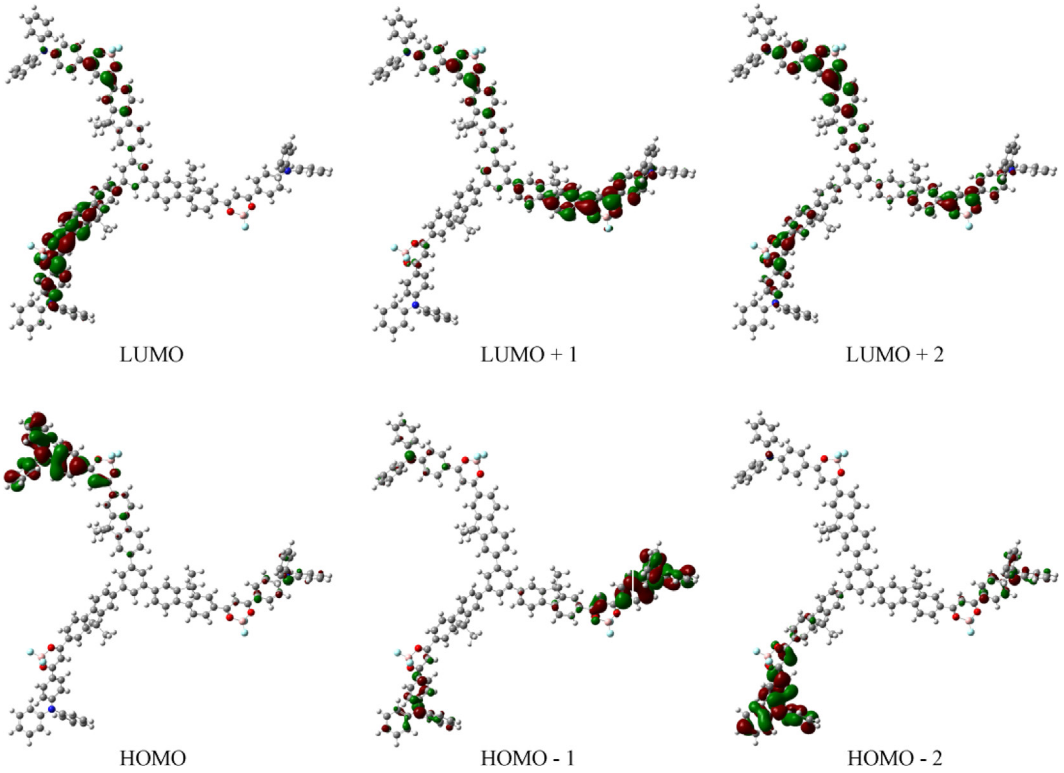

Fig. 5. The molecular orbital surfaces in the optimized ground-state structure for (**TBF**)$_3$**Ph**.

toluene with Φ_F of 0.73 and 0.67, respectively, and strong red light emitting in solid states was also detected for (**TBC**)$_3$**Ph** and (**TBF**)$_3$**Ph** with Φ_F of 0.36 and 0.27, respectively. The electrochemical data illustrated that they had considerably higher electron affinities than AlQ_3, which indicated that they could be used as electron-transporting materials. Therefore, the two difluoroboron β-diketonate complexes (**TBC**)$_3$**Ph** and (**TBF**)$_3$**Ph** might have potential applications as electron-transporters and emitting materials.

Table 3
Main orbital transitions calculated with TD-DFT

Complex	λ_{abs}[a]/nm	λ_{calcd}[b]/nm	f[c]	Composition (%)[d]
(**TBC**)$_3$Ph	486	484.4	2.1102	H→L (35) H-1→L+1 (21) H-2→L (21)
		482.8	1.5531	H→L+2 (32) H-1→L+1 (24) H-1→L+2 (16) H-2→L+2 (6) H→L (6)
(**TBF**)$_3$Ph	490	494.2	1.6190	H→L+2 (34) H-2→L (24) H→L (13) H→L+1 (10) H-1→L+1 (8)
		493.5	2.1576	H-1→L+1 (32) H-2→L (22) H-1→L+2 (16) H-2→L+1 (10) H→L+2 (7)

[a] Experimental maximum absorption in toluene.
[b] Calculated electronic transition band in vacuo.
[c] Calculated oscillator strength in vacuo.
[d] H represents HOMO, L represents LUMO.

4. Experimental

4.1. Materials and measurements

Toluene was freshly distilled from sodium and benzophenone under nitrogen. CH_2Cl_2 was distilled from CaH_2. All the other chemicals and reagents were used as received from commercial sources without further purification. ^{1}H NMR spectra were recorded on a Bruker Avance III 500 MHz and 400 MHz, and Varian 300 MHz using $CDCl_3$ or DMSO-d_6 as solvents. ^{13}C NMR spectra were recorded on Bruker Avance III 125 MHz and 100 MHz using $CDCl_3$ or DMSO-d_6 as solvents. UV–vis absorption spectra were determined on a Shimadzu UV-1601PC spectrophotometer. Fluorescent emission spectra were carried out on a Shimadzu RF-5301 luminescence spectrometer. The quantum yields of the samples in solid states were measured by an Edinburgh Instrument FLS920 using an integrating sphere with the excitation wavelength of 500 nm. Mass spectra were performed on Agilent 1100 MS series and AXIMA CFR MALDI/TOF (matrix assisted laser desorption ionization/time-of-flight) MS (COMPACT). C, H, and N analyses were taken on a Vario EL cube elemental analyzer. Cyclic voltammetry was carried out with a CHI 604B electrochemical working station at room temperature under N_2 atmosphere at a scan rate of 100 mV/s. A three electrode configuration was used for the measurement: a platinum electrode as the working electrode, a platinum wire as the counter electrode, and an Ag/$AgNO_3$ electrode as the reference electrode. Ferrocene was used as external reference. A solution of Bu_4NPF_6 (0.1 M) in CH_2Cl_2 was used as the supporting electrolyte.

4.2. Synthesis

Compounds **1**,[29] **4**,[30] methyl 4-(diphenylamino)benzoate,[31] and 1,3,5-tris(4,4,5,5-tetramethyl-1,3,2-dioxaborolan-2-yl)benzene[32] were synthesized according to the literature.

*4.2.1. 1-(6-Bromo-9-dodecyl-9H-carbazol-3-yl)ethanone (**2**).* Acetyl chloride (2.05 mL, 29.0 mmol) was added slowly to a suspension of $AlCl_3$ (3.88 g, 29.0 mmol) in 1,2-dichloroethane in ice bath over 20 min. Then, the solution of compound **1** (8.0 g, 19.3 mmol) in 1,2-dichloroethane was added slowly. After that, the ice bath was removed, and the dark green slurry was refluxed overnight. After cooling, the mixture was poured into water and extracted with dichloromethane for three times. Then the organic phase was combined and dried over anhydrous Na_2SO_4. Removing the solvent under reduced press, the residue was purified by column chromatography (silica gel, CH_2Cl_2/petroleum ether, v/v=2/1) to give a white solid (4.60 g). Yield: 52%. Mp: 104.0–106.0 °C. ^{1}H NMR (500 MHz, $CDCl_3$, ppm): δ 8.68 (d, J=1.5 Hz, 1H), 8.26 (d, J=2.0 Hz, 1H), 8.16–8.13 (m, 1H), 7.60–7.57 (m, 1H), 7.40 (d, J=8.5 Hz, 1H), 7.31 (d, J=8.5 Hz, 1H), 4.29 (t, J=7.5, 7.0 Hz, 2H), 2.72 (s, 3H), 1.88–1.82 (m, 2H), 1.36–1.22 (m, 18H), 0.87 (t, J=7.0, 7.0 Hz, 3H) (Fig. S4). ^{13}C NMR (100 MHz, $CDCl_3$, ppm): δ 197.4, 143.4, 139.7, 129.1, 126.9, 124.9, 123.4, 122.1, 121.5, 112.8, 110.7, 108.7, 43.5, 31.9, 29.5, 29.3, 28.9, 27.2, 26.6, 22.7, 14.1 (Fig. S5). Elemental analysis for $C_{26}H_{34}BrNO$, calcd: (%) C, 68.41; H, 7.51; N, 3.07. Found: (%) C, 68.23; H, 7.65; N, 3.10. MALDI-TOF MS, m/z (%): calcd for 456.2 $[M+H]^+$, 458.2 $[M+H]^+$, found: 456.7 (100) $[M+H]^+$, 458.7 (100) $[M+H]^+$ (Fig. S6).

*4.2.2. 1,1′,1″-(6,6′,6″-(Benzene-1,3,5-triyl)tris(9-dodecyl-9H-carbazole-6,3-diyl))triethanone (**3**).* A mixture of 1,3,5-tris(4,4,5,5-tetramethyl-1,3,2-dioxaborolan-2-yl)benzene (0.20 g, 0.44 mmol), compound **2** (0.78 g, 1.71 mmol), and K_2CO_3 (0.60 g, 4.4 mmol) in distilled water (20 mL) and toluene (20 mL) was charged and bubbled by nitrogen for 15 min, then $Pd(PPh_3)_4$ (20 mg) was added. The mixture was refluxed for 24 h under nitrogen. After cooling to room temperature, the mixture was extracted with dichloromethane for three times. Then the organic phase was combined and dried over anhydrous Na_2SO_4. Removing the solvent under reduced press, the residue was purified by column chromatography (silica gel, petroleum ether/ethyl acetate, v/v=3/1) to give a light yellow oil (0.14 g). Yield: 27%. ^{1}H NMR (500 MHz, $CDCl_3$, ppm): δ 8.85 (d, J=1.5 Hz, 3H), 8.58 (d, J=1.5 Hz, 3H), 8.18–8.16 (m, 3H), 8.06 (s, 3H), 8.01–7.99 (m, 3H), 7.59 (d, J=8.5 Hz, 3H), 7.46 (d, J=8.5 Hz, 3H), 4.39 (t, J=7, 7 Hz, 6H), 2.74 (s, 9H), 1.97–1.92 (m, 6H), 1.44–1.24 (m, 54H), 0.86 (t, J=6.5, 7.5 Hz, 9H) (Fig. S7). ^{13}C NMR (100 MHz, $CDCl_3$, ppm): δ 197.6, 143.6, 142.9, 140.8, 133.6, 128.9, 126.5, 126.2, 124.9, 123.8, 122.7, 122.1, 119.3, 109.6, 108.5, 53.4, 43.5, 31.9, 29.5, 29.4, 29.3, 29.0, 27.3, 26.6, 22.6, 14.1 (Fig. S8). Elemental analysis for $C_{84}H_{105}N_3O_3$, calcd: (%)C, 83.74; H, 8.78; N, 3.49. Found: (%) C, 83.63; H, 8.65; N, 3.57. MALDI-TOF MS, m/z (%): calcd for 1205.8 $[M+H]^+$, found: 1206.0 (100) $[M+H]^+$ (Fig. S9).

*4.2.3. 1-(7-Bromo-9,9-dioctyl-9H-fluoren-2-yl)ethanone (**5**).* By following the synthetic procedure for compound **2**, compound **5** was prepared from compound **4** (13.77 g, 29.33 mmol) and acetyl chloride (3.11 mL, 43.99 mmol) catalyzed by $AlCl_3$ (5.87 g, 43.99 mmol). The crude product was purified by column chromatography (silica gel, petroleum ether/CH_2Cl_2 v/v=2/1) to give a white solid (7.20 g). Yield: 48%. Mp: 70.0–72.0 °C. ^{1}H NMR (400 MHz, $CDCl_3$, ppm): δ 7.95 (d, J=8.8 Hz, 2H), 7.72 (d, J=7.6 Hz, 1H), 7.61 (d, J=8.0 Hz, 1H), 7.49 (d, J=6.8 Hz, 2H), 2.66 (s, 3H), 2.05–1.90 (m, 4H), 1.22–1.03 (m, 20H), 0.81 (t, J=6.8, 7.2 Hz, 6H), 0.58–0.50 (m, 4H) (Fig. S10). ^{13}C NMR (100 MHz, $CDCl_3$, ppm): δ 197.9, 154.1, 150.7, 144.9, 138.8, 136.2, 130.3, 128.3, 126.4, 122.6, 122.4, 122.0, 119.5, 55.6, 40.0, 31.7, 29.8, 29.1, 26.8, 23.7, 22.6, 14.0 (Fig. S11). Elemental analysis for $C_{31}H_{43}BrO$. Calcd: (%) C, 72.78; H, 8.47. Found: (%) C, 72.89; H, 8.55. MALDI-TOF MS, m/z (%): calcd for 511.3 $[M+H]^+$, 513.3 $[M+H]^+$, found: 511.1 (98) $[M+H]^+$, 513.1 (100) $[M+H]^+$ (Fig. S12).

*4.2.4. 1,1′,1″-(Benzene-1,3,5-triyltris(9,9-dioctyl-9H-fluorene-7,2-diyl))triethanone (**6**).* By following the synthetic procedure for compound **3**, compound **6** was prepared from compound **5** (0.88 g, 1.71 mmol) and 1,3,5-tris(4,4,5,5-tetramethyl-1,3,2-dioxaborolan-2-yl)benzene (0.20 g, 0.44 mmol) catalyzed by $Pd(PPh_3)_4$ (20 mg) in the presence of K_2CO_3 (0.60 g, 4.4 mmol). The crude product was purified by column chromatography (silica gel, petroleum ether/ethyl acetate, v/v=10/1) to give a white solid (0.21 g). Yield: 35%. Mp: 54.0–56.0 °C. ^{1}H NMR (300 MHz, $CDCl_3$, ppm): δ 8.01–7.99 (m, 6H), 7.91 (d, J=7.8 Hz, 6H), 7.83–7.77 (m, 6H), 7.72 (s, 3H), 2.69 (s, 9H), 2.09 (t, J=6.6, 6.9 Hz, 12H), 1.18–1.06 (m, 60H), 0.78 (t, J=6.6, 7.2 Hz, 18H), 0.73–0.58 (m, 12H) (Fig. S13). ^{13}C NMR (100 MHz, $CDCl_3$, ppm): δ 198.1, 152.9, 151.3, 145.6, 142.8, 141.3, 139.5, 135.9, 128.3, 126.6, 125.5, 122.5, 121.9, 121.1, 119.6, 55.5, 40.2, 31.7, 29.9, 29.2, 26.8, 23.8, 22.6, 14.0 (Fig. S14). Elemental analysis for $C_{99}H_{132}O_3$. Calcd: (%) C, 86.79; H, 9.71. Found: (%) C, 86.80; H, 9.81. MALDI-TOF MS, *m*/*z* (%): calcd for 1371.0 $[M+H]^+$, found: 1371.5 (100) $[M+H]^+$ (Fig. S15).

*4.2.5. 6,6′,6″-(6,6′,6″-(Benzene-1,3,5-triyl)tris(9-dodecyl-9H-carbazole-6,3-diyl))tris(4-(4-(diphenylamino)phenyl)-2,2-difluoro-2H-1,3,2-dioxaborinin-1-ium-2-uide) ((**TBC**)$_3$**Ph**).* Sodium hydride (60%, 0.12 g, 3.00 mmol) was added quickly to a dry flask containing a solution of compound **3** (0.30 g, 0.25 mmol) and methyl 4-(diphenylamino)benzoate (0.46 g, 1.51 mmol) in toluene (30 mL). The reaction mixture was refluxed under an atmosphere of nitrogen for 24 h. The solution was cooled to the room temperature and then acidified with dilute HCl and extracted with CH_2Cl_2 for three times. The organic phase was combined and dried over anhydrous Na_2SO_4. After removal of solvent, the residue was used directly in the next step without purification. Then, the solution of 3,3′,3″-(6,6′,6″-(benzene-1,3,5-triyl)tris(9-dodecyl-9*H*-carbazole-6,3-diyl))tris(1-(4-(diphenylamino)phenyl)propane-1,3-dione) in dry CH_2Cl_2 (30 mL) was heated to reflux under an atmosphere of nitrogen, and excess $BF_3\cdot Et_2O$ (0.5 mL) was added. The mixture was refluxed for 12 h. After the solvent was removed, the residue was purified by column chromatography (silica gel, CH_2Cl_2/petroleum ether, v/v=3/1) to afford (**TBC**)$_3$**Ph** (100 mg) as a bright red solid. Yield: 18%. Mp: 198.0–200.0 °C. ^{1}H NMR (500 MHz, DMSO-d_6, 60 °C, ppm): δ 9.30 (d, J=1 Hz, 3H), 8.87 (s, 3H), 8.38–8.36 (m, 3H), 8.17 (s, 3H), 8.13–8.10 (m, 9H), 7.84–7.81 (m, 6H), 7.65 (s, 3H), 7.36 (t, J=8.0, 7.5 Hz, 12H), 7.21–7.17 (m, 18H), 6.82 (d, J=9.0 Hz, 6H), 4.54 (t, J=6.5, 6.5 Hz, 6H), 1.90–1.85 (m, 6H), 1.35–1.12 (m, 54H), 0.76 (t, J=6.5, 7.5 Hz, 9H) (Fig. S16). ^{13}C NMR (125 MHz, DMSO-d_6, 60 °C, ppm): δ 180.6, 179.1, 153.9, 145.6, 145.1, 142.6, 141.2, 133.9, 131.2, 130.3, 127.2, 126.9, 126.2, 124.8, 123.6, 123.5, 123.1, 122.9, 120.1, 118.4, 110.9, 110.5, 92.6, 43.5, 31.6, 29.4, 29.3, 29.2, 29.0, 28.9, 22.3, 14.1 (Fig. S17). Elemental analysis for $C_{141}H_{141}B_3F_6N_6O_6$. Calcd: (%) C, 78.33; H, 6.57; N, 3.89. Found: (%) C, 78.56; H, 6.43; N, 3.60. MALDI-TOF MS, *m*/*z* (%): calcd for 2143.1 $[M-F+H]^+$, 2162.1 $[M+H]^+$, found: 2143.8 (100) $[M-F+H]^+$, 2162.5 (28) $[M+H]^+$ (Fig. S18).

*4.2.6. 6,6′,6″-(Benzene-1,3,5-triyltris(9,9-dioctyl-9H-fluorene-7,2-diyl))tris(4-(4-(diphenylamino)phenyl)-2,2-difluoro-2H-1,3,2-dioxaborinin-1-ium-2-uide) ((**TBF**)$_3$**Ph**).* By following the synthetic procedure for the complex (**TBC**)$_3$**Ph**, (**TBF**)$_3$**Ph** was prepared from compound **6** (0.40 g, 0.29 mmol), methyl 4-(diphenylamino)benzoate (0.53 g, 1.75 mmol), 60% sodium hydride (0.14 g, 3.50 mmol), and $BF_3\cdot Et_2O$ (0.5 mL). The crude product was purified by column chromatography (silica gel, CH_2Cl_2/petroleum ether, v/v=2/1) to afford (**TBF**)$_3$**Ph** (78 mg) as a dark red solid. Yield: 12%. Mp: 158.0–160.0 °C. ^{1}H NMR (500 MHz, $CDCl_3$, ppm): δ 8.13–8.09 (m, 6H), 8.03 (d, J=9.0 Hz, 6H), 7.93 (t, J=2.5, 5.0 Hz, 6H), 7.86 (d, J=7.0 Hz, 3H), 7.82–7.80 (m, 3H), 7.73 (s, 3H), 7.39 (t, J=8.0, 8.0 Hz, 12H), 7.26–7.22 (m, 18H), 7.10 (s, 3H), 7.01 (d, J=9.0 Hz, 6H), 2.12 (t, J=6.5, 6.5 Hz, 12H), 1.17–1.06 (m, 60H), 0.77 (t, J=7.0, 7.0 Hz, 18H), 0.67–0.64 (m, 12H) (Fig. S19). ^{13}C NMR (100 MHz, $CDCl_3$, ppm): δ 180.4, 180.0, 154.2, 153.2, 151.8, 147.2, 145.4, 142.7, 141.8, 139.3, 131.3, 131.0, 129.9, 128.1, 126.6, 125.9, 125.6, 122.8, 122.7, 121.9, 121.4, 120.1, 118.5, 92.2, 55.8, 40.3, 31.7, 29.9, 29.2, 29.1, 23.8, 22.5, 14.0 (Fig. S20). Elemental analysis for $C_{156}H_{168}B_3F_6N_3O_6$. Calcd: (%) C, 80.50; H, 7.28; N, 1.81. Found: (%) C, 80.38; H, 7.20; N, 1.98. MALDI-TOF MS, *m*/*z* (%): calcd for 2307.6 (100) $[M-F]^+$, 2326.6 $[M]^+$, found: 2307.9 (100) $[M-F]^+$, 2326.6 (16) $[M]^+$ (Fig. S21).

Acknowledgements

This work was supported by the National Natural Science Foundation of China (_501100001809) (51073068, 21374041), Open Project of State Key Laboratory of Supramolecular Structure and Materials (SKLSSM201407), and Open Project of State Key Laboratory of Theoretical and Computational Chemistry (K2013-02).

Supplementary data

Supplementary data associated with this article can be found in the online version, at http://dx.doi.org/10.1016/j.tet.2014.03.069. These data include MOL files and InChiKeys of the most important compounds described in this article.

References and notes

1. Rao, Y. L.; Wang, S. *Inorg. Chem.* **2011**, *50*, 12263.
2. Li, D.; Zhang, H. Y.; Wang, Y. *Chem. Soc. Rev.* **2013**, *42*, 8416.
3. Loudte, A.; Burgess, K. *Chem. Rev.* **2007**, *107*, 4891.
4. Xu, S. P.; Evans, R. E.; Liu, T. D.; Zhang, G. Q.; Demas, J. N.; Trindle, C. O.; Fraser, C. L. *Inorg. Chem.* **2013**, *52*, 3597.
5. Ono, K.; Yoshikawa, K.; Tsuji, Y.; Yamaguchi, H.; Uozumi, R.; Tomura, M.; Taga, K.; Saito, K. *Tetrahedron* **2007**, *63*, 9354.
6. Felouat, A.; D'Aléo, A.; Fages, F. *J. Org. Chem.* **2013**, *78*, 4446.
7. Tanaka, K.; Tamashima, K.; Nagai, A.; Okawa, T.; Chujo, Y. *Macromolecules* **2013**, *46*, 2969.
8. (a) Cogné-Laage, E.; Allemand, J. F.; Ruel, O.; Baudin, J.; Croquette, V.; Blanchard-Desce, M.; Jullien, L. *Chem.—Eur. J.* **2004**, *10*, 1445; (b) Halik, M.; Wenseleers, W.; Grasso, C.; Stellacci, F.; Zojer, E.; Barlow, S.; Brédas, J.; Perry, J. W.; Marder, S. R. *Chem. Commun.* **2003**, 1490.
9. (a) Zhang, G. Q.; Lu, J. W.; Sabat, M.; Fraser, C. L. *J. Am. Chem. Soc.* **2010**, *132*, 2160; (b) Sun, X. X.; Zhang, X. P.; Li, X. Y.; Liu, S. Y.; Zhang, G. Q. *J. Mater. Chem.* **2012**, *22*, 17332; (c) Nguyen, N. D.; Zhang, G. Q.; Lu, J. W.; Sherman, A. E.; Fraser, C. ,L. *J. Mater. Chem.* **2011**, *21*, 8409; (d) Liu, T. D.; Chien, A. D.; Lu, J. W.; Zhang, G. Q.; Fraser, C. L. *J. Mater. Chem.* **2011**, *21*, 8401; (e) Zhang, G. Q.; Singer, J. P.; Kooi, S. E.; Evans, R. E.; Thomas, E. L.; Fraser, C. L. *J. Mater. Chem.* **2011**, *21*, 8295.
10. Poon, C. T.; Lam, W. H.; Wong, H. L.; Yam, V. W. *J. Am. Chem. Soc.* **2010**, *132*, 13992.
11. Sun, Y. M.; Rohde, D.; Liu, Y. Q.; Wan, L. J.; Wang, Y.; Wu, W. P.; Di, C. G.; Yu, G.; Zhu, D. B. *J. Mater. Chem.* **2006**, *16*, 4499.
12. (a) Zhang, X. F.; Lu, R.; Jia, J. H.; Liu, X. L.; Xue, P. C.; Xu, D. F.; Zhou, H. P. *Chem. Commun.* **2010**, 8419; (b) Zhang, X. F.; Liu, X. L.; Lu, R.; Zhang, H. J.; Gong, P. *J. Mater. Chem.* **2012**, *22*, 1167; (c) Liu, X. L.; Xu, D. F.; Lu, R.; Li, B.; Qian, C.; Xue, P. C.; Zhang, X. F.; Zhou, H. P. *Chem.—Eur. J.* **2011**, *17*, 1660; (d) Liu, X. L.; Zhang, X. F.; Lu, R.; Xue, P. C.; Xu, D. F.; Zhou, H. P. *J. Mater. Chem.* **2011**, *21*, 8756; (e) Qian, C.; Cao, K. Y.; Liu, X. L.; Zhang, X. F.; Xu, D. F.; Xue, P. C.; Lu, R. *Chin. Sci. Bull.* **2012**, *57*, 4264.
13. (a) Qiu, X. P.; Lu, R.; Zhou, H. P.; Zhang, X. F.; Xu, T. H.; Liu, X. L.; Zhao, Y. Y. *Tetrahedron Lett.* **2008**, *49*, 7446; (b) Qiu, X. P.; Lu, R.; Zhou, H. P.; Zhang, X. F.; Xu, T. H.; Liu, X. L.; Zhao, Y. Y. *Tetrahedron Lett.* **2007**, *48*, 7582.
14. Wang, J. L.; He, Z. C.; Wu, H. B.; Cui, H. B.; Li, Y.; Gong, Q. H.; Cao, Y.; Pei, J. *Chem.—Asian J.* **2010**, *5*, 1455.
15. Zhang, W. B.; Jin, W. H.; Zhou, X. H.; Pei, J. *Tetrahedron* **2007**, *63*, 2907.
16. (a) Zhou, H. P.; Zhao, X.; Huang, T. H.; Lu, R.; Zhang, H. Z.; Qi, X. H.; Xue, P. C.; Liu, X. L.; Zhang, X. F. *Org. Biomol. Chem.* **2011**, *9*, 1600; (b) Zhou, H. P.; Lu, R.; Zhao, X.; Qiu, X. P.; Xue, P. C.; Liu, X. L.; Zhang, X. F. *Tetrahedron Lett.* **2010**, *51*, 5287.
17. (a) Jiang, Y. H.; Wang, Y. C.; Hua, J. L.; Tang, J.; Li, B.; Qian, S. X.; Tian, H. *Chem. Commun.* **2010**, 4689; (b) Wang, B.; Wang, Y. C.; Hua, J. L.; Jiang, Y. H.; Huang, J. H.; Qian, S. X.; Tian, H. *Chem.—Eur. J.* **2011**, *17*, 2647.
18. Sun, Y. M.; Xiao, K.; Liu, Y. Q.; Wang, J. L.; Pei, J.; Yu, G.; Zhu, D. B. *Adv. Funct. Mater.* **2005**, *15*, 818.
19. Zhao, C.; Wakamiya, A.; Inukai, Y.; Yamaguchi, S. *J. Am. Chem. Soc.* **2006**, *128*, 15934.
20. Sonntag, M.; Strohriegl, P. *Chem. Mater.* **2004**, *16*, 4736.
21. (a) Yiu, A. T.; Beaujuge, P. M.; Lee, O. P.; Woo, C. H.; Toney, M. F.; Frechet, J. M. J. *J. Am. Chem. Soc.* **2012**, *134*, 2180; (b) Xu, T. H.; Lu, R.; Liu, X. L.; Zheng, X. Q.; Qiu, X. P.; Zhao, Y. Y. *Org. Lett.* **2007**, *9*, 797.
22. Anderson, J. D.; McDonald, E. M.; Lee, P. A.; Anderson, M. L.; Ritchie, E. L.; Hall, H. K. *J. Am. Chem. Soc.* **1998**, *120*, 9646.
23. Domercq, B.; Grasso, C.; Maldonado, J. L.; Halik, M.; Barlow, S.; Marder, S. R.; Kippelen, B. *J. Phys. Chem. B* **2004**, *108*, 8647.

24. (a) Zhan, Y.; Cao, K. Y.; Xue, P. C.; Lu, R. *Tetrahedron Lett.* **2013**, *54*, 594; (b) Jia, J. H.; Cao, K. Y.; Xue, P. C.; Zhang, Y.; Zhou, H. P.; Lu, R. *Tetrahedron* **2012**, *68*, 3626; (c) Tang, J.; Hua, J. L.; Wu, W. J.; Li, J.; Jin, Z. G.; Long, Y. T.; Tian, H. *Energy Environ. Sci.* **2010**, *3*, 1736.
25. Frisch, M. J.; Trucks, G. W.; Schlegel, H. B.; Scuseria, G. E.; Robb, M. A.; Cheeseman, J. R.; Scalmani, G.; Barone, V.; Mennucci, B.; Petersson, G. A.; Nakatsuji, H.; Caricato, M.; Li, X.; Hratchian, H. P.; Izmaylov, A. F.; Bloino, J.; Zheng, G.; Sonnenberg, J. L.; Hada, M.; Ehara, M.; Toyota, K.; Fukuda, R.; Hasegawa, J.; Ishida, M.; Nakajima, T.; Honda, Y.; Kitao, O.; Nakai, H.; Vreven, T.; Montgomery, T. A.; Peralta, J. E., Jr.; Ogliaro, F.; Bearpark, M.; Heyd, J. J.; Brothers, E.; Kudin, K. N.; Staroverov, V. N.; Kobayashi, R.; Normand, J.; Raghavachari, K.; Rendell, A.; Burant, J. C.; Iyengar, S. S.; Tomasi, J.; Cossi, M.; Rega, N.; Millam, J. M.; Klene, M.; Knox, J. E.; Cross, J. B.; Bakken, V.; Adamo, C.; Jaramillo, J.; Gomperts, R.; Stratmann, R. E.; Yazyev, O.; Austin, A. J.; Cammi, R.; Pomelli, C.; Ochterski, J. W.; Martin, R. L.; Morokuma, K.; Zakrzewski, V. G.; Voth, G. A.; Salvador, P.; Dannenberg, J. J.; Dapprich, S.; Daniels, A. D.; Farkas, O.; Foresman, J. B.; Ortiz, J. V.; Cioslowski, J.; Fox, D. J. *Gaussian 09, Revision A.02*; Gaussian: Wallingford, CT, 2009.
26. Zhang, W. W.; Mao, W. L.; Hu, Y. X.; Tian, Z. Q.; Wang, Z. L.; Meng, Q. J. *J. Phys. Chem. A* **2009**, *113*, 9997.
27. Lin, Z. H.; Bjorgaard, J.; Yavuz, A. G.; Köse, M. E. *J. Phys. Chem. C* **2011**, *115*, 15097.
28. Xue, P. C.; Xu, Q. X.; Gong, P.; Qian, C.; Zhang, Z. Q.; Jia, J. H.; Zhao, X.; Lu, R.; Ren, A. M.; Zhang, T. R. *RSC Adv.* **2013**, *3*, 26403.
29. Pansay, S.; Prachumrak, N.; Jungsuttiwong, S.; Keawin, T.; Sudyoadsuk, T.; Promarak, V. *Tetrahedron Lett.* **2012**, *53*, 4568.
30. Poriel, C.; Rault-Berthelot, J.; Thirion, D.; Barrière, F.; Vignau, L. *Chem.—Eur. J.* **2011**, *17*, 14031.
31. Gujadhur, R.; Venkataraman, D.; Kintigh, J. T. *Tetrahedron Lett.* **2001**, *42*, 4791.
32. Bao, B. Q.; Yuwen, L. H.; Zhan, X. W.; Wang, L. H. *J. Polym. Sci., Part A: Polym. Chem.* **2010**, *48*, 3431.